LA-UR -86-1490

CONF-860612--5

RECEIVED BY OSTI MAY 12 1986

MASTER

TITLE MEASUREMENT OF PERFORMANCE LIMITS IN CRYOGENIC HEAT PIPES

LA-UR--86-1490

DE86 010208

AUTHOR(S) Friedrich Haug
F. Coyne Prenger
Robert H. Chrisman

SUBMITTED TO AIAA/ASME 4th Joint Thermophysics and Heat Transfer Conference
June 2-4, 1986
Boston, MA

Los Alamos Los Alamos National Laboratory
Los Alamos, New Mexico 87545

MEASUREMENT OF PERFORMANCE LIMITS IN CRYOGENIC HEAT PIPES

by

Friedrich Haug
Los Alamos National Laboratory
Los Alamos, NM

F. Coyne Prenger
Astronautics Technology Center
Madison, WI

and

Robert H. Chrisman
Los Alamos National Laboratory
Los Alamos, NM

ABSTRACT

This paper describes the results of an experimental study designed to investigate the fabrication and operation of gravity-assist cryogenic heat pipes. Two heat pipes were built, the first having no formal wick but a roughened internal surface, the second having spiral grooves machined with a specially developed tool. The wall material of the heat pipes was brass and hydrogen was used as the working fluid. The wicked heat pipe became operational over the entire temperature range from the triple-point to the critical point. The performance limitation depended on the operating temperature and the tilt angle. Axial heat flux densities of up to 50W/cm^2 were obtained.

NOMENCLATURE

A_e	evaporator heat transfer area
A_v	vapor flow cross-sectional area
E_t	dimensionless entrainment parameter
h_{fg}	latent heat of vaporization
K	ratio groove width to thread width
L	heat pipe length
p_v	vapor pressure
Q	heat pipe power
Q_E	dimensionless power
q	axial heat flux density
R_i	radius of vapor flow channel
R_o	radius of vapor flow channel plus wick depth ($R_i + \delta$)
V_ℓ	liquid volume of fluid inventory
V_p	liquid volume of pool
V_t	total volume of heat pipe interior
V_v	volume of vapor flow area
V_w	volume of grooves in wick structure
δ	wick depth
σ	surface tension
ρ_v	vapor density
ρ_ℓ	liquid density

1. INTRODUCTION

There has been a considerable number of investigations of high and ambient temperature heat pipes in the last years and accordingly, the design technique and operating characteristics of these heat pipes are now reasonably well understood. By comparison, the gravity assisted, cryogenic heat pipe has not yet been extensively studied. A theoretical analysis of cryogenic heat pipes is given by Chi[1]. The first experimental study with a cryogenic heat pipe using nitrogen as a working fluid was carried out by Haskin[2]. In his experiments, large temperature drops of up to 20K were observed which were partially attributed to the low thermal conductance of liquid nitrogen in the wick.

In subsequent experiments[3] with a nitrogen heat pipe of total length 25cm and one cm diameter at a power of 5 watts a temperature drop of 17K over the entire length was found, which confirms the results of Haskin[2]. Using an elaborate wick structure consisting of a wrapped core for axial liquid transport, radial flow legs and secondary wicking at the wall[4], a reasonably good isothermal operating condition was obtained. Brennan et. al.[5], investigated an arterial and grooved nitrogen heat pipe at close to horizontal orientation. Alario et. al.[6], developed a re-entrant groove hydrogen heat pipe using extrusion technology. An excess vapor reservoir was provided at the evaporator to minimize the pressure in the containment during ambient storage. Testing of this heat pipe[7] showed that the heat pipe became operational at temperatures between 20-30K. Axial heat flux densities in the vapor passage of up to 9.3 W/cm^2 were obtained. The heat pipe design and the wick structures were relatively elaborate.

The main objective of the present study is to simplify the design for small cryogenic heat pipes, especially the wick structure, so that fabrication cost can be reduced and heat pipe utilization increased. For this study, two heat pipes were built, the first having no formal wick but a roughened internal surface or "orange peel" and the second having spiral grooves machined with a specially developed tool[8]. Hydrogen was used as a working fluid. The heat pipes were tested in the gravity-assisted mode varying both the tilt angle and operating temperature to investigate their performance characteristics. A description of the heat pipes, the development of the wick structure, the experimental techniques, and the results are presented.

2. HEAT PIPE DESIGNS

Copper, which has been used as the wall material for cryogenic heat pipe experiments, exhibits extremely high thermal conductivity in the temperature range investigated in this study. Therefore, since the axial thermal conduction would contribute significantly to the axial heat transfer and make it difficult to study the heat transfer due to the two-phase vapor transport, brass was used for fabricating the heat pipes in this investigation. It has a very small thermal conductivity at liquid hydrogen temperatures and is also compatible with hydrogen. The two heat pipes were fabricated using oversized brass tubing that was drawn to the required diameter.

Fig. 1. View of the Internal Surface of the Wickless Heat Pipe after Drawing.

2.1 Heat Pipe #1 ("Orange Peel")

A simple heat pipe can be made by using a tube with an unwicked or roughened inner surface (wickless heat pipe). This was tried as a first approach in this investigation. The oversized brass tubing with a smooth inner wall surface having an o.d. of 4.76mm and a wall thickness of 0.81mm was drawn to the desired size of 3.29mm o.d. which left an i.d. of 1.65mm. The comparatively large wall thickness minimized the pressure containment hazard during ambient storage. After drawing, the originally smooth surface on the inner diameter exhibited a wrinkled appearance which resembled an "orange peel" as shown in Fig. 1. The heat pipe was provided with a small pinch-off tube for evacuation and filling of the working fluid. The filling procedure is described in a later section. The overall length of the heat pipe was 160mm.

2.2 Heat Pipe #2 (Spiral Grooves)

Recently a new method of wicking small diameter heat pipes was developed at LANL[8]. The tool used for internal threading is three pointed and is shaped so as to produce spiral grooves in the i.d. of the tube wall. The tool (see Fig. 2)

Fig. 2. Tool for Internal Threading.

is fed through the tube. Figure 3 shows a sample of the three-pitch threads in a brass tube with an i.d. of 3.14mm. Generally wicking of small diameter heat pipes is difficult. However, this method showed excellent results with fairly large upsets of the tube wall. This wick is similar to one obtained by using the invention of Runyan and Grover[9]. A groove depth of 0.18mm was obtained with a groove spacing of 0.18mm. There were 32 grooves per centimeter. Additional tests have shown that groove depths of up to 0.28mm with a spacing of only 0.10mm could be obtained with this tool.

Fig. 3. Sample of the 3.14mm i.d. Tubing after Threading.

After wicking the oversized tube was drawn to the desired diameter, following the same procedure for the wickless heat pipe (orange peel) described above. The geometry changed slightly due to the drawing process. The wick depth essentially remained the same while the groove spacing increased to 0.25mm due to the elongation of the tube.

2.3 Filling

For convenience the heat pipes were filled with hydrogen above its critical point rather than with the liquid phase. This method required special care to achieve the desired fluid inventory because of the large temperature and pressure changes involved.

A. Fluid Inventory. In most applications, the amount of fluid inventory is chosen so that the wick structure of the heat pipe is saturated and some excess fluid, which will form a pool in the evaporator section during operation, is included. This technique was used in this study. The total volume of the heat pipe interior is

$$V_t = V_v + V_w \qquad (1)$$

where V_v is the volume of the vapor channel and V_w the volume of the wick, which cannot be neglected in these small diameter pipes with comparatively deep grooves. The volume of the wick is

$$V_w = \pi(R_0^2 - R_1^2)\,KL \qquad (2)$$

where K is the ratio of the groove width to the groove pitch. The liquid volume is

$$V_\ell = V_w + V_p \qquad (3)$$

Any closed cycle heat pipe operation is basically an isochoric process i.e., the mean density of the fluid remains constant in the enclosure. Using conservation of mass a mean density of the fluid can be determined

$$\bar{\rho} = (V_\ell/V_t)(\rho_\ell - \rho_g) + \rho_g \qquad (4)$$

Because the operating temperature range of a hydrogen heat pipe is small (13-33K), it can be shown that the liquid volume ratio V_ℓ/V_t doesn't change appreciably, therefore the liquid volume remains nearly constant during heat pipe operation. Because of the limited pressure of the hydrogen source available, the heat pipe was cooled to liquid nitrogen temperatures at ambient pressure during filling. Using (4) and the ideal gas relation the pressure of hydrogen at liquid nitrogen temperature can be determined.

B. Procedure. Before filling, the heat pipe was cleaned with a solvent and evacuated at ambient temperature for several hours at a pressure of 10⁻ Torr using a diffusion vacuum pump. Then the heat pipe was immersed in liquid nitrogen and pressurized with hydrogen to the desired value. Heat Pipe #1 (orange peel) was filled with two different quantities of working fluid. For Heat Pipe #2 the fluid inventory was sufficient to saturate the wick, leaving only a small amount of excess liquid for the pool.

3. EXPERIMENTS

3.1 Test Set Up and Instrumentation

It was intended to operate the heat pipes in the gravity-assisted mode and to vary the tilt angle and operating temperature. Figure 4 shows the basic set-up of the heat pipe test apparatus. The heat pipe was heated with a direct contact electrical heater (Heater #1). The condenser section of the heat pipe was soldered into a copper cylinder by means of a cold solder eutectic of Gallium and Indium which is liquid at room temperature and solidifies at temperatures below 16°C thus insuring uniform thermal contact between the heat pipe condenser and the copper cylinder. The copper cylinder was attached and thermally bonded to the cryotip of a helium gas cycle refrigerator which provided temperatures as low as 10K. The cooling capacity of the refrigerator and the temperature of its cryotip depended on the heat load and could not directly be controlled. The method used to control the heat pipe temperature was via an auxiliary heater (Heater #2) mounted onto the copper cylinder. This heater supplied a parasitic heat load to the host refrigerator thus indirectly controlling its cold side temperature. External thermocouples were used to measure temperature differences along the heat pipe wall. A carbon-glass resistor was used for the reference temperature. Chromel/Gold wire combination was used for the thermocouples because of its superior sensitivity with respect to other material combinations over

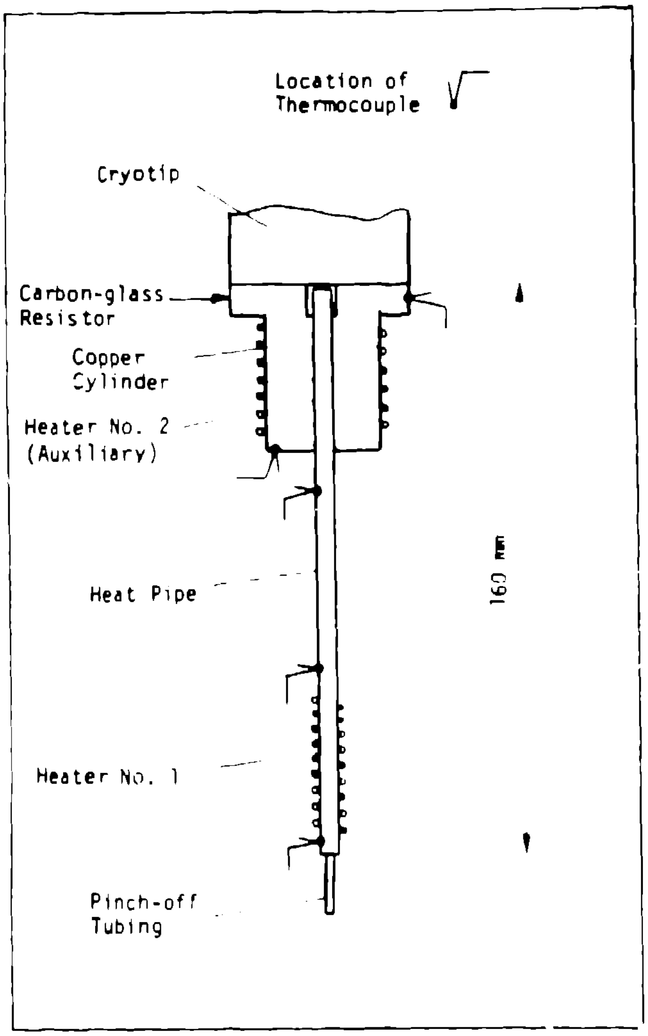

Fig. 4. Heat Pipe Test Apparatus and Instrumentation

the temperature range of 10 to 30K. However, special care was taken in the fabrication of these thermocouple junctions. The oxidized surface layers on the wires of the thermocouple junction could cause a "tunneling"[10] of free electrons from one leg to another at the thermocouple junction and would, therefore, lead to an erroneously higher voltage. The reading would show a higher "apparent temperature" than the true value. This effect is usually not noticeable at ambient temperatures because of the dominance of Brownian movement. However, at the temperature range investigated in this study this effect can lead to voltages that deviate considerably from the Seebeck voltage. The following method was used to fabricate nearly oxide-free solder joints. In order to break up the oxide layer at the Chromel wire a high temperature acid flux and Indium solder was used to carefully tin this leg. To avoid amalgamation of the Gold wire a low temperature solder was used for its tinning. Both legs were then soldered together to form the thermocouple junction using the low temperature solder without melting the higher temperature solder on the Chromel leg. Using the reference carbon-glass resistor calibration of the thermocouples showed good results. The test apparatus was insulated with multilayer insulation and installed in a vacuum chamber.

3.2 Tests

Heat Pipe #1 was initially tested with a fairly small liquid pool. In subsequent tests, a large pool covering almost the entire length of the evaporator section was used. The fluid inventory of Heat Pipe #2 was sufficient to saturate the wicks during operation leaving a fairly small pool. Heat pipe operating temperature was controlled by heat input to the auxiliary Heater #2 at the copper cylinder. Heat pipe power was controlled via Heater #1 and increased in small increments. The temperature along the heat pipe, the reference temperature, and the respective heat loads to the heaters were recorded in intervals of 30 seconds.

The performance limit of the heat pipe was obtained when an uncontrollable temperature excursion occurred i.e., the temperatures at the beginning of the evaporator and subsequently the temperatures in the adiabatic section would rapidly and continuously increase. This resulted from complete dry-out of the evaporator. The operating temperature was varied to find the temperature range in which the heat pipe could function and to "map" the performance characteristics in this range. Several operating regimes were observed and are discussed in the next section.

4. RESULTS AND DISCUSSION

4.1 Heat Pipe #1 (Orange Peel)

The wickless heat pipe was difficult to operate and would carry only very small heat loads i.e., in the 10mW range, which can be attributed to axial conduction in the enclosure wall. Even at these small powers a slow, but uncontrollable excursion would occur indicating a performance limit. An explanation could be that vapor bubbles are generated in the liquid pool of the evaporator section, which increase in size and cause a two-phase slug flow. The expanding vapor bubbles in the small 1.6mm i.d. tubing would push the liquid towards the condenser and the condensate would accumulate there. This process would be repeated until the evaporator is dried out and a temperature excursion would set in leading to a failure in the heat pipe operation. The experiments were repeated several times and always showed the same results.

4.2 Heat Pipe #2 (Spiral Grooves)

Heat Pipe #2, was tested with one fill charge, at different operating temperatures, and at different tilt angles. Figure 5 shows the performance characteristic of the heat pipe for a tilt angle of 15° measured from the horizontal. At an operating temperature close to the triple point, the performance is limited to approximately 35mW. With increasing temperature the limit increases with a fairly gradual slope to temperatures of approximately 27K. A maximum performance occurs at a temperature of 29K. At this tilt angle and at relatively small heat pipe powers accurate data was difficult to obtain, especially at temperatures greater than 30K. At these temperatures the heat pipe would operate under nonisothermal conditions, i.e., the temperature at the beginning of the evaporator would be elevated with respect to the temperature in the adiabatic section. This has been studied in more detail at larger tilt angles where higher performance is expected.

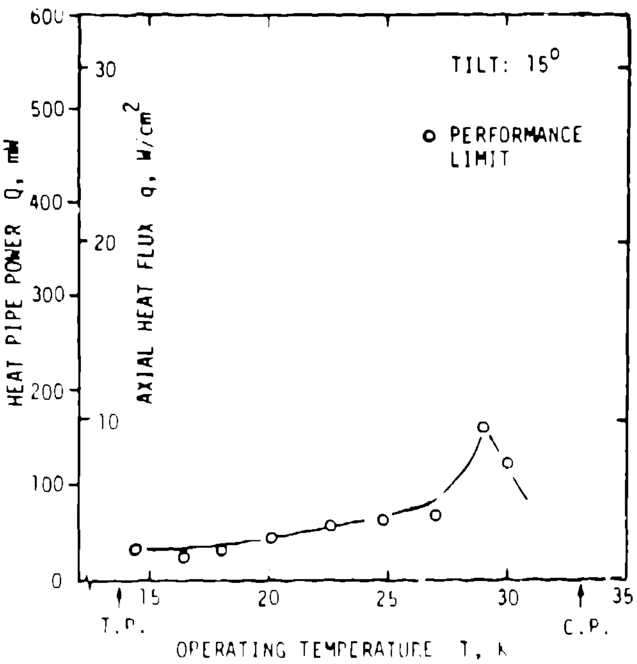

Fig. 5. Heat Pipe Power and Axial Heat Flux Versus Operating Temperature at 15° Tilt.

At a tilt angle of 30° (Fig. 6) the performance limits are generally twice as high as at 15°. Basically, the performance limit increases with increasing temperatures and reaches a maximum close to 400mW at temperatures around 28-29K. The data indicate that the heat pipe becomes operational over the entire temperature range, from the triple point (T.P.) to the critical point (C.P.). This is remarkable since in other investigations[7], the heat pipe becomes operational over a temperature interval of only 20-30K. At temperatures close to the triple point the performance limit increases rapidly with temperature. At temperatures above 14.4K the increase is very small. This seems to indicate that two different performance limits exist which have a transition point close to 14.4K.

At operating temperatures between 22 and 28K a surprising operation mode was observed. Even well below the performance limit the temperature at the beginning of the evaporator would increase to a value several degrees above the saturation temperature in the adiabatic section. However, it was found that this nonisothermal operation would not necessarily lead to a complete dry-out and subsequent limitations in performance. Instead temperature at the beginning of the evaporator would drop close to the saturation temperature and then increase again, indicating a rewetting and a subsequent dry-out, respectively. The amplitude of the temperature fluctuation increased with increasing heat pipe power until the performance limit was reached where the temperature in the evaporator increased steadily indicating a permanent dry-out. In Fig. 6, data between approximately 22 to 28K and 100mW, indicate the separation between isothermal operation which lie below the data and the nonisothermal operation which lie above it. At

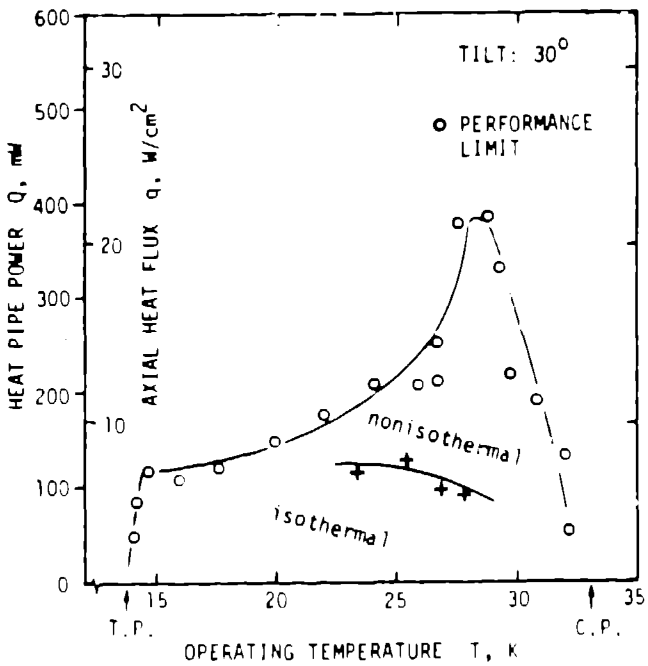

Fig. 6. Heat Pipe Power and Axial Heat Flux Versus Operating Temperature at 30° Tilt. Areas of Isothermal and Nonisothermal Heat Pipe Operation are Indicated.

operating temperatures above 28K the temperature fluctuations decreased markedly and were hardly noticeable. At operating temperatures below 22K, no temperature fluctuation was observed and the heat pipe operated isothermally until the performance limit was reached. This kind of behavior probably existed also at the 15° tilt angle, but due to the very small heat pipe power and small temperature fluctuations this could not be observed.

Figure 7 shows the performance limit and various isothermal and nonisothermal areas of heat pipe operation at a tilt of 60°. As in the previous discussion of the data at 30° tilt it can be noted that the heat pipe becomes operational at temperatures close to the triple-point and that the performance limit increases steeply at fairly low temperatures. At approximately 14.6K the performance limit is almost 300mW. At increasing temperatures the gradient decreases slightly, but is still fairly high. At temperatures of around 24 to 25K a maximum in performance is obtained which is approximately 900mW or 50W/cm². At still higher operating temperatures the performance limit drops sharply towards zero near the critical point. Also, in this test isothermal and nonisothermal operation characteristics were observed. At temperatures below 20K the heat pipe operated isothermally until the limit was reached. At higher

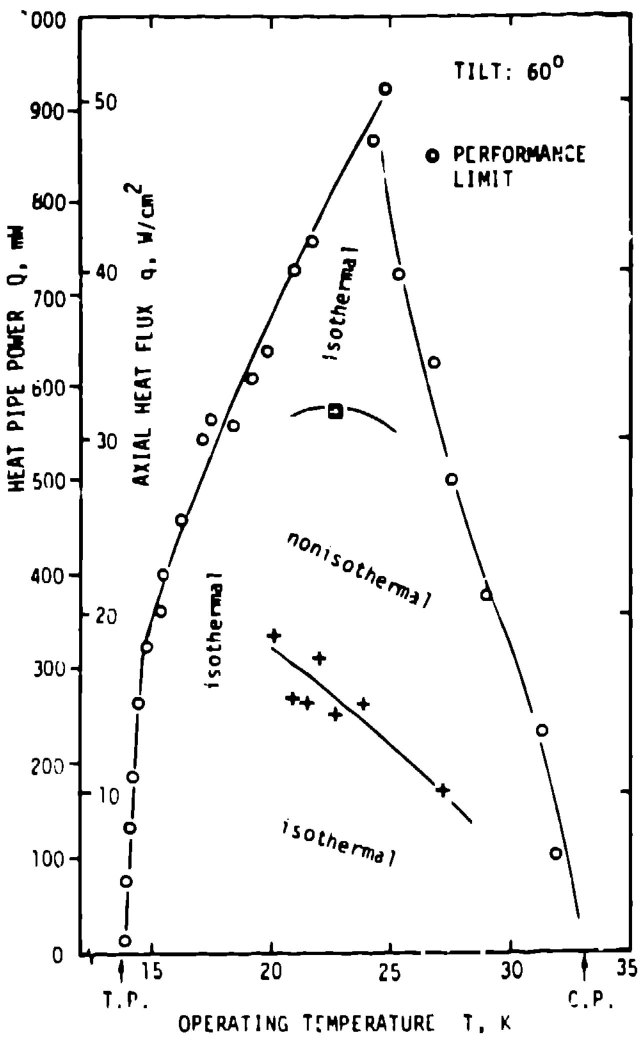

Fig. 7. Heat Pipe Power and Axial Heat Flux Versus Operating Temperature for 60° Tilt. Areas of Isothermal and Nonisothermal Heat Pipe Operation are Indicated.

temperatures the isothermal operation area lie under a curve that starts at around 300mW and 20K and ends at approximately 180mW and 27K. Above this curve the heat pipe operates nonisothermally with temperature fluctuations in the evaporator section that can exceed 10K. At still larger heat pipe powers, it was observed that the heat pipe could fall back to an isothermal operation which is called, "Recovery from Non isothermal Operation." The heat pipe operated isothermally until the performance limit was reached. Four areas of operation were distinguished, three being isothermal, and one being nonisothermal.

Figure 8 shows the performance characteristic of the heat pipe operated in the vertical position. The same behavior can be found as in the previous discussions; a steep increase in performance with increasing temperatures, a maximum of approximately 600mW at 23K and a decrease in performance as the critical point is approached. The maximum power obtained is approximately 30% smaller than at 60° tilt. Also in this case, four different areas of operation were found which correspond in temperature range to the data at 60° tilt.

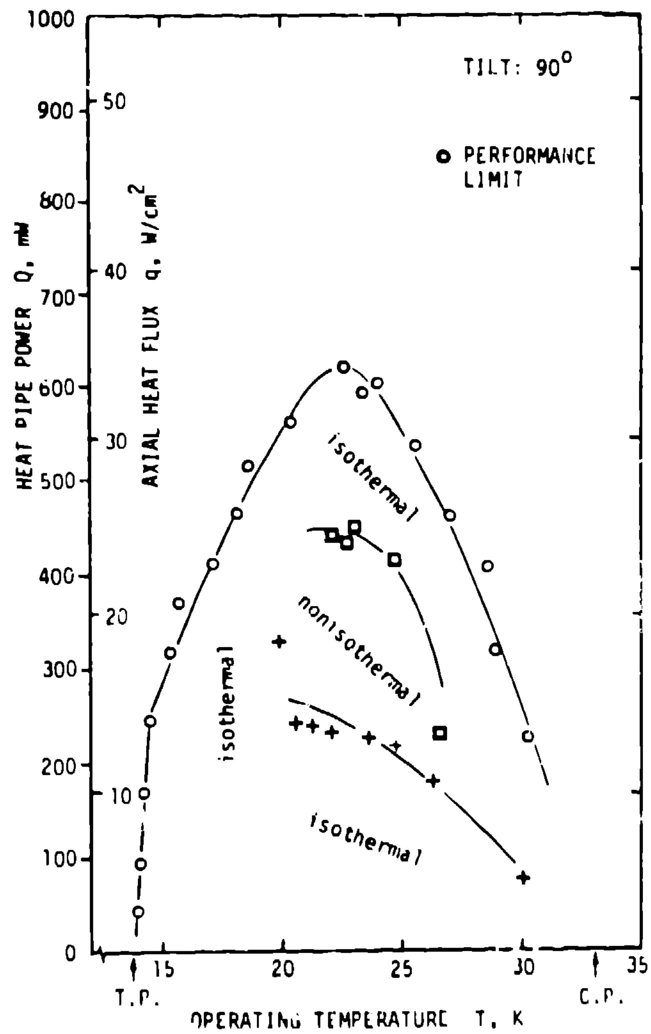

Fig. 8. Heat Pipe Power and Axial Heat Flux Versus Operating Temperature for 90° Tilt (vertical). Areas of Isothermal and Nonisothermal Heat Pipe Operation are Indicated.

Figure 9 is a summary of the data at 30°, 60°, and 90° (vertical) tilt. In all three cases, the performance increases steeply with increasing temperatures close to the triple point. In this region the three curves lie practically together. This is an indication that the limitations are independent of tilt angle. It is possible due to the very small vapor pressure in this temperature range that the sonic limit is encountered. This limit is described by

$$Q = 0.474\, A_v h_{fg} (\rho_v P_v)^{0.5} \qquad (5)$$

and is proportional to the square root of the vapor density. In the figure the curve representing the sonic limit is almost a vertical line which corresponds well with the experimental data. At increasing temperatures the three curves separate and a decrease in gradient occurs, which is especially pronounced at the 30° tilt operation indicating a different type of limit. At temperatures of about 29K the three curves unite again and the performance limit drops to zero at close to the critical point. Again, in this temperature range, the performance limit is independent of tilt angle. A decreasing limit with temperature is characteristic of a boiling limit. A critical radial heat flux is calculated by using a correlation by Rohsenhow and Griffith[11].

$$Q = 0.012\, h_{fg} \rho_v A_e \left(\frac{\rho_\ell - \rho_v}{\rho_v}\right)^{0.6} \qquad (6)$$

This boiling limit prediction is shown in Fig. 9. This correlation provides only an upper limit to the test data and does not include any geometric effects.

Between the temperature range of approximately 14.5K to 25K a different type of limitation may exist. Since the heat pipe performance limit depends on the tilt angle, it is presumed that the limitation predominantly is a liquid return limit. This can be induced by the vapor/liquid interaction of the counter flowing vapor which could lead to entrainment or flooding in the condenser of the heat pipe. An entrainment or flooding limit correlation for vertical heat pipes based on an interface stability model[12] and verified by experimental data[13] is given by

$$Q_e = C E_t^{1/2} \qquad (7)$$

and

$$C = 33.7\delta \qquad (8)$$

and δ is the characteristic depth of the surface texturing in cm. The dimensionless variables are

$$F_t = \frac{\rho}{\rho_v h_{fg} \delta} \qquad (9)$$

and

$$Q_e = \frac{Q}{\rho_v h_{fg}^{1.5} A_v} \qquad (10)$$

However, this correlation over-predicts the data for Heat Pipe #2. Flooding limits can be higher for non-vertical operation due to the existence of puddle flow which decreases the interfacial area.

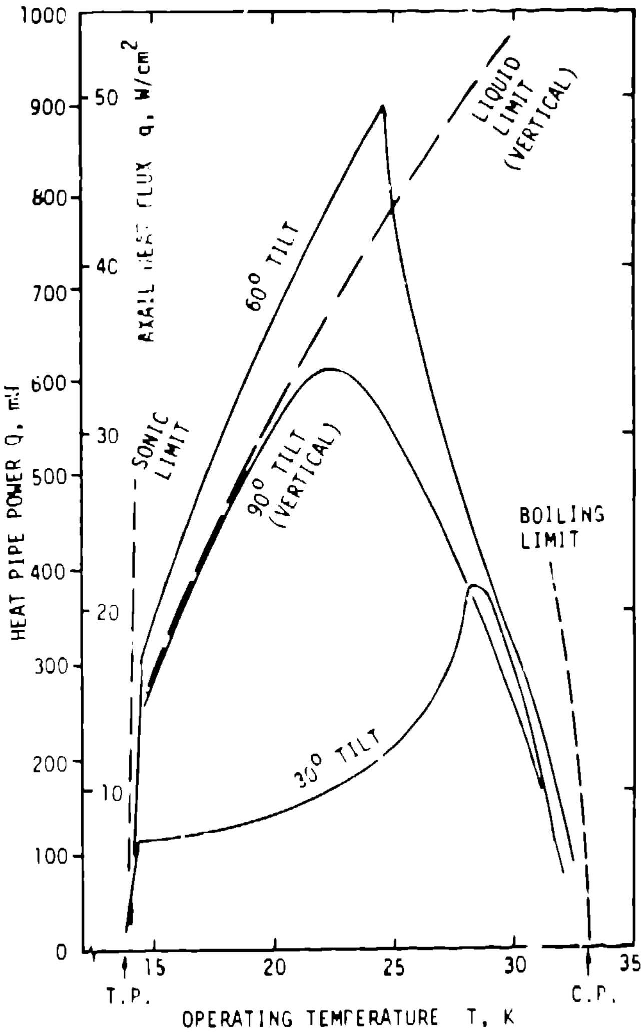

Fig. 9. Comparison of Measured Performance Limits at Different Inclinations with Performance Predictions.

In addition to the possibility for entrainment or flooding in the heat pipe a liquid limit has also been postulated[14] and has been observed in liquid metal heat pipes[15]. This mechanism is based on a liquid flow impedance within the wick structure. Preliminary analysis of the data for Heat Pipe #2 indicates experimental verification of the liquid limit model as shown in Fig. 9.

CONCLUSIONS

A new method to wick small bore diameter tubings with circumferential grooves has been introduced. Fabrication costs can be reduced and heat pipe utilization increased using this method. Two 1.6mm i.d. heat pipes with hydrogen as working fluid were built, the first being a wickless heat pipe, the second having spiral grooves. The wickless heat was difficult to operate and would carry only small heat loads, i.e. in the 10mW range. The heat pipe with spiral grooves became operational practically over the entire temperature range from the triple-point to the critical point, i.e. from 13.8K to 32.9K. Generally, the performance limit increased with increasing temperature and reached a maximum at temperatures between 24-29K depending on the tilt angle. At a small tilt angle of 15° the highest limit was approximately 150mW. With an increase in tilt angle the performance limit increased and a maximum was found at 60° tilt which was 900mW or 50W/cm^2 axial heat flux. In the vertical position the performance limits were approximately 30% smaller than at 60° tilt. At very small operating temperatures and at temperatures close to the critical point the performance limit was independent of inclination. An analysis of the experimental data indicates that at very small operating temperatures a sonic limit exists. At temperatures close to the critical point a boiling limitation might occur. In the medium temperature range the performance limit depends strongly on the tilt angle which indicates a limitation due to liquid flow impedance within the wick structure. A recently postulated liquid limit model agrees well with the experimental data obtained in the vertical position.

REFERENCES

1. Chi, S.W., Cygnarowicz, T.A., "Theoretical Analysis of Cryogenic Heat Pipes," ASME Paper No. 70-HT/SpT-6, 1970.

2. Haskin, W.L., "Cryogenic Heat Pipe," Technical Report AFFDS-TR-66-228, 1967.

3. Kissner, G.L., "Development of a Cryogenic Heat Pipe, "Proceedings of the First International Heat Pipe Conf.," Stuttgart, 1973.

4. Nelson, B.E., Petrie, W., "Experimental Evaluation of a Cryogenic Heat Pipe Radiator in a Vacuum Chamber," Proceedings of the First International Heat Pipe Conf., Stuttgart, 1973.

5. Brennan, P., et. al., "Arterial and Grooved Cryogenic Heat Pipes," ASME Paper No. 71-WA/HT-42, 1971.

6. Alario, F., Kosson, R., McCreight, C., "A Re-Entrant Groove Hydrogen Heat Pipe," AIAA Paper No. 78-420, 1978.

7. Alario, F., Kosson, R., "Performance Testing of a Hydrogen Heat Pipe," AIAA Paper No. 80-0212, 1980.

8. Chrisman, R.H., "Upsetting Tool for Internal Threading of Small Tubes to be Used as Heat Pipes," Patent Application, Los Alamos National Laboratory, 1985.

9. Runyan, J.E., Grover, G.M., "Heat Pipe and Method and Apparatus for Fabricating Same," United States Patent No. 3,753,364, 1973.

10. Fisher, J.C., Giaever, I., "Tunneling Through Thin Insulating Layers," Journal of Applied Physics (1961), Vol. 32, No. 2, pp. 172-177.

11. Dunn, P.D., Reay, D.A., "Heat Pipes," Pergamon Press, London, Third Edition, pp. 56.

12. Prenger, F. C. "Performance Limits of Gravity-Assisted Heat Pipes," Fifth International Heat Pipe Conf., Tsukuba, Japan, May 1984.

13. Prenger, F.C., Kemme, J. E.," Performance Limits of Gravity-Assist Heat Pipes with Simple Wick Structures," Proceedings of the Fourth International Heat Pipe Conf., London, 1981, pp. 137-146.

14. Prenger, F. C., "Liquid Limit Model for Gravity-Assisted Heat Pipes," Sixth International Heat Pipe Conf., Grenoble, France, May 1987 (in preparation).

15. Prenger, F. C., Keddy, E. S., and Sena, J. T., "Performance Characteristics of Gravity-Assisted, Potassium Heat Pipes," AIAA 20th Thermophysics Conf., Williamsburg, VA, June 1985.